# Investigation of plasma wall interactions between tungsten plasma facing components and helium plasmas in the WEST tokamak

E. Tsitrone, B. Pegourie, J.P. Gunn, E. Bernard, V. Bruno, Y. Corre, L. Delpech, M. Diez, D. Douai, A. Ekedahl, et al.

**ACCEPTED MANUSCRIPT**

# Investigation of plasma wall interactions between tungsten plasma facing components and helium plasmas in the WEST tokamak

To cite this article before publication: Emmanuelle Tsitrone *et al* 2021 *Nucl. Fusion* in press https://doi.org/10.1088/1741-4326/ac2ef3

# INVESTIGATION OF PLASMA WALL INTERACTIONS BETWEEN TUNGSTEN PLASMA FACING COMPONENTS AND HELIUM PLASMAS IN THE WEST TOKAMAK

E. TSITRONE
CEA, Institute for Research on Fusion by Magnetic confinement, 13108 Saint-Paul-Lez-Durance, France
emmanuelle.tsitrone@cea.fr

B. PEGOURIE, J. P. GUNN, E. BERNARD, V. BRUNO, Y. CORRE, L. DELPECH, M. DIEZ, D. DOUAI, A. EKEDAHL, N. FEDORCZAK, A. GALLO, T. LOARER, S. VARTANIAN
CEA, Institute for Research on Fusion by Magnetic confinement, 13108 Saint-Paul-Lez-Durance, France

J. GASPAR, M. LE BOHEC, F. RIGOLLET
Aix Marseille Univ, CNRS, IUSTI, Marseille, France

R. BISSON
Aix-Marseille Univ, CNRS, PIIM, UMR 7345, Marseille F-13397, France

S. BREZINSEK, T. DITTMAR
Forschungszentrum Jülich, Insitut für Energie und Klimaforschung - Plasmasphysik, Jülich, Germany

G. DE TEMMERMAN
ITER Organization, CS 90 046, 13067 St.-Paul-lez-Durance Cedex, France

A. HAKOLA
VTT, P.O.Box 1000, 02044 VTT, Finland

T. WAUTERS
Laboratory for Plasma Physics, LPP-ERM/KMS, B-1000 Brussels, Belgium

M. BALDEN, M. MAYER
Max-Planck-Institut für Plasmaphysik, Garching, Germany

WEST Team*, see http://west.cea.fr/WESTteam

**Abstract**

ITER will operate with a tungsten divertor, a material featuring surface morphology changes when exposed to helium plasmas, in particular the formation of the so called tungsten fuzz under specific conditions. Investigating interactions between tungsten plasma facing components and helium plasmas in a tokamak environment is therefore a key point to consolidate predictions for the ITER divertor performance and lifetime. To this end, a dedicated helium campaign was performed in the full tungsten WEST tokamak, cumulating ~2000 s of repetitive L mode discharges. It is shown that conditions for tungsten fuzz formation, as derived from linear devices experiments (incident helium energy $E_{inc}$ > 20 eV, helium fluence > $10^{24}$ He/m$^2$, surface temperature $T_{surf}$ > 700°C), were met in the outer strike point area of the inertially cooled tungsten divertor elements of WEST. Preliminary inspection of the components after the campaign did not show visible signs of surface modification, but points to significant net erosion in the outer strike point area. An extensive post mortem analysis is now ongoing to confirm these first indications. These results underline that the complex balance between erosion /redeposition (in particular linked to impurities) and tungsten fuzz formation needs to be taken into account in tokamak conditions.

## 1. INTRODUCTION

ITER will be equipped with a tungsten divertor, which is planned to operate over a significant period of time (~10 years, cumulating more than 2000 hours of plasma exposure [1]), from the Pre-Fusion Power Operation phase into the Fusion Power Operation phase [2]. As was shown in a number of linear devices as well as in tokamaks, tungsten (W) exhibits pronounced surface morphology changes under helium (He) plasma exposure, which can affect its thermal and mechanical properties (see [3] and references therein). In particular, He induced nanostructures, such as He nanobubbles or the so-called W fuzz, can be formed at the W surface, depending on plasma conditions and surface temperature. Helium operation is planned in the ITER Pre-Fusion Power Operation phase, in order to demonstrate H mode operation without activating the in-vessel components [2]. Helium will also be present during the Fusion Power Operation phase, as ash from the D-T reaction. Investigating interactions between W plasma facing components and He plasmas in a tokamak environment is therefore a key point to consolidate predictions for the ITER divertor performance and lifetime.

This paper reports on a He campaign performed to investigate these issues in the full tungsten tokamak WEST. Section 2 describes the configuration of the WEST tungsten divertor during the He campaign, while

section 3 gives an overview of the He plasma scenario performed. Section 4 discusses local divertor plasma parameters obtained during the He campaign and where they stand with respect to conditions for W fuzz formation. Finally, section 5 presents the first observations carried out on the W divertor of WEST after the He exposure.

## 2. WEST : A FULL TUNGSTEN TOKAMAK

WEST is a Mega-Ampere class superconducting device targeted at testing ITER tungsten divertor in a tokamak environment [4]. To this end, the lower divertor of WEST was progressively equipped with ITER like divertor Plasma Facing Units (PFU). The ITER like PFU of WEST are based on the ITER divertor technology (actively cooled tungsten monoblocks (MB) assembled on a copper heat sink [5]). During the first phase of WEST operation, 5 experimental campaigns were performed (C1 to C5 over 2017-2020), with the He campaign executed at the end of the C4 campaign in 2019. During this phase, the lower divertor was made of a mix of ITER like PFU and W coated inertially cooled PFU (called inertial PFU in this paper). The inertial PFU are made of 15 µm thick W coatings on a graphite substrate with a 3 µm thick Mo interlayer [6]. The W coated PFU include an inner and outer tile, while the ITER like PFU are made of a single element. This is illustrated in Figure 1 showing the divertor configuration of WEST for phase 1, with a mix of ITER like PFU and inertial PFU. The coordinates system used along the PFU in this paper (see sections 3 and 4) is also described in Figure 1.

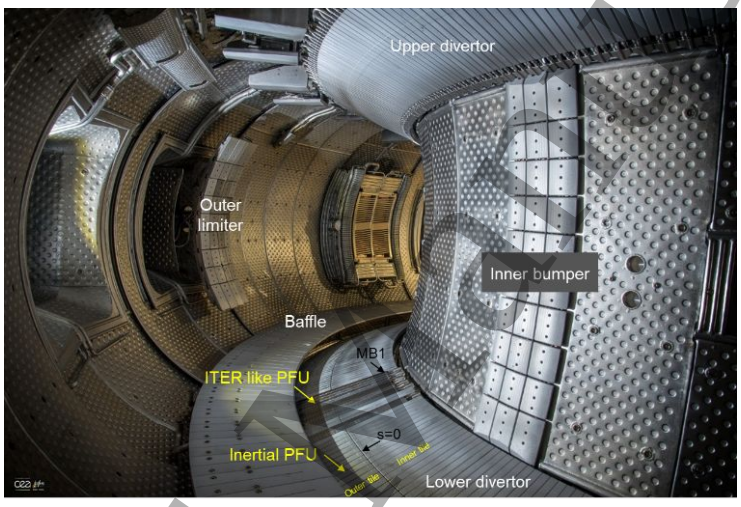


*Figure 1: picture of the WEST vessel during phase 1 operation (before the start of the C3 campaign in 2018), showing the lower divertor equipped with a mix of ITER like actively cooled bulk W PFU and inertial W coated PFU. The main plasma facing components are indicated in white (lower and upper divertor, baffle, inner bumper and outer limiter). The ITER like PFU and the inertial PFU are indicated in yellow, showing the inner and outer tile for the inertial PFU. The coordinate system used in the paper is also shown in black. The s coordinate used for the IR data analysis starts from the High Field Side of the outer tile of inertial PFU. The monoblock (MB) coordinate used for Langmuir probe analysis starts on MB1 of the ITER like PFU on the High Field Side and goes up to MB35 on the Low Field Side. ( ©C.Roux/CEA )*

WEST was also equipped with a set of 8 erosion marker tiles [7], where on top of the 15 µm W coatings of the inertial PFU were added a 100 nm thick Mo interlayer and a 2 to 4 µm thick W layer. These erosion marker tiles were located in areas of maximum plasma loading in the ripple pattern (see description of the WEST ripple pattern below for more details). 2 erosion markers PFU were dismantled for analysis at the end of C3 campaign (deuterium exposure only) and 2 additional ones were dismantled at the end of the C4 campaign, where He operation was performed. Analysis is still ongoing [8], but first results are discussed in section 5.

In order to carry out plasma wall interactions studies, a comprehensive set of plasma edge and divertor diagnostics is available in WEST. In particular, standard and very high resolution infra-red (IR) cameras are installed to monitor the lower divertor surface temperature [9][10]. They are complemented by embedded diagnostics, such as thermocouples and optical fibers equipped with Fiber Bragg Gratings [11][12]. In addition, an array of divertor Langmuir probes measures local plasma parameters (particle flux, density, electron temperature) [13].

In WEST, it should be noted that the divertor heat and particle fluxes on the divertor are modulated by the ripple, through a periodic modulation of the magnetic field lines incidence angle. This results in areas of maximum and minimum heat and particle loads alternating on the High Field Side (HFS) and Low Field Side (LFS) in the region of the Inner Strike Point (ISP) and Outer Strike Point (OSP) respectively. This is illustrated for instance on the IR divertor view in Figure 4. In addition, as evidenced in a number of tokamaks, there is a in / out asymmetry in

WEST divertor profiles, with higher steady state power loads observed on the LFS [14]. As a result, the highest loads are concentrated at the position of the OSP poloidally and the position corresponding to the maximum in the ripple pattern toroidally, as indicated on Figure 4 with the label "max OSP". In the following sections, this area of maximum divertor load is referred to as max OSP and is the main zone of interest to investigate He-W plasma wall interactions.

## 3. OVERVIEW OF THE HE CAMPAIGN

### 3.1. Main objectives of the first He campaign in WEST

The main objective of this first He campaign was to investigate divertor PFU surface morphology changes stemming from the interaction between W and He plasmas. In particular, the aim was to explore phenomena expected in a medium to high surface temperature range, such as the formation of He nanobubbles (expected above 600-700 K) and W fuzz (expected in a range of 900-1900 K) (see figure 7 in [3]). In order to do so, the strategy was to run repetitive long pulses (20-30 s) to cumulate He exposure on the inertial PFU of the lower divertor. Indeed, the inertial PFU undergo significant temperature excursion during the shot, allowing to reach relevant temperature for W surface morphology changes, in contrast with the ITER like PFU, which keep a constant (and lower) surface temperature after a few seconds, thanks to active cooling.

The campaign was targeted to reach parameters allowing for W fuzz formation in the max OSP area, namely as described in [3] :

- an incident He energy above 20 eV (but lower than ~350 eV to avoid competition with erosion, as illustrated in figure 8 of [3])
- PFU surface temperature above 900 K (and below 1900 K)
- He fluence above the seed fluence required for W fuzz formation (> $10^{24}$ He/m$^2$)

A He phase of ~1 week was carried out at the end of the C4 campaign, to allow for PFU post mortem analysis immediately after He exposure.

### 3.2. Plasma scenario for the He campaign

A robust L mode plasma scenario heated by Lower Hybrid (LH) power was designed to cumulate significant He fluence on the lower divertor within the 4 days of He operation allocated at the end of the C4 campaign (8 sessions run in double shifts). The selected discharge parameters ($I_p$=300 kA, average density 4 $10^{19}$ m$^{-3}$, $P_{LH}$ ~ 4 MW, medium pulse length in the range 20-30 s), corresponding to a loop voltage $V_{loop}$ ~ 200 mV, allowed keeping a high pulse repetition rate and avoiding MHD issues related to operation at low loop voltage ($V_{loop}$ < 50 mV). These parameters, in particular in terms of pulse length, were also chosen to allow significant temperature excursion of the inertial PFU above the temperature where W fuzz formation can be expected (900K).
A D prefill was used throughout most of the He campaign, as it was identified to be a more robust start up scenario than He prefill and to have a weak impact on the He content of the plasma during flat top. Nitrogen ($N_2$) injection was also used in the start-up phase of the discharge (between 0 and 3 s). This initial phase is indeed critical in tokamaks with metallic walls, since heavy impurities can radiate in the plasma core and generate MHD unstable plasmas [16]. The $N_2$ injection had to be adjusted to variable levels throughout the 4 days of experiments to avoid MHD in the start-up phase of the discharge, and W related MHD was the main operational issue encountered, as is also the case for D operation in WEST. The density and the LH heating power ramp up also had to be fine tuned in the early phase of the discharge. Steady state flat top conditions are typically reached after 10 s.
Roughly ~140 successful discharges, cumulating ~2000 s of plasma exposure and 4.4 GJ of injected energy, were performed. A boronisation was performed on the day before the start of the He experiments, but no boronisation was run during the He campaign to avoid strong variations in the vessel wall conditions. After a few shots performed for change over between D and He (typically ~10 shots, see [15] for more details on He to D changeover in WEST), the He/($D_2$+He) ratio, as measured from optical Penning gauge spectroscopy in the exhaust gas, was typically above 90% and up to 95% during the discharge flat top, despite the D prefill.
Figure 2 illustrates typical parameters for a shot of the He campaign in terms of plasma current, density and temperature. The injected and radiated power are also shown, with a radiated fraction higher in He than in D operation (in the range 60-65% in He to be compared with ~50% in D). Finally, gas injection (D prefill, $N_2$ injection in the early phase of the discharge and He injection) is presented, as well as exhausted gas. Particle balance was performed up to 30 s after the end of the pulse. It shows that a significant amount of He is trapped in the vessel walls during the pulse (2/3 of injected He is trapped in the wall at the end of the discharge shown in

Figure 2), and is not fully recovered during post pulse outgassing up to 30s. He is also seen to outgas more rapidly than D, suggesting different release mechanisms [15].

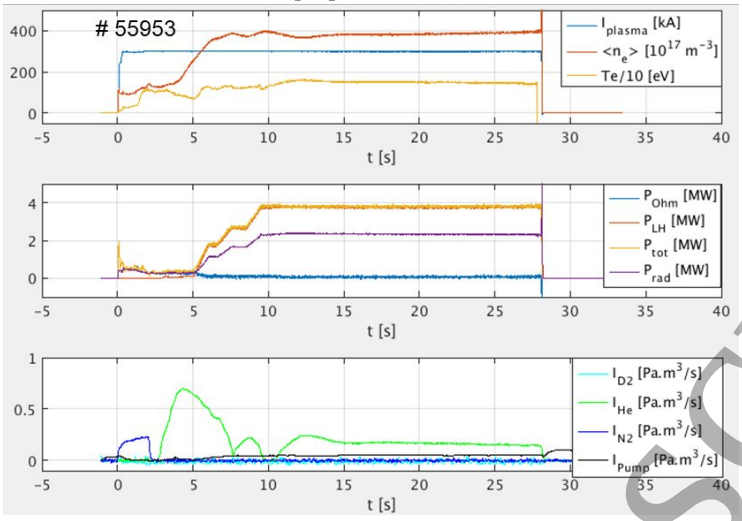


*Figure 2: plasma parameters for a typical shot of the He campaign (#55953), with a) plasma current, density and core electron temperature b) total power, LH power, radiated power and ohmic power and c) injection rate of $D_2$ (prefill), He and $N_2$ as well as particle flux exhausted by the pumps.*

Local divertor plasma parameters were measured by Langmuir probes, and are shown in Figure 3. At the OSP, the incident He particle flux is around 1.8 $10^{22}$ He/$m^2$/s (calculated assuming a pure $He^{++}$ flux impinging on the divertor) while the electron temperature is around 30 eV. It can also be noted from Figure 3 that the peak in particle flux and electron temperature is found to be in good agreement with the strike point position reconstruction at the OSP, while the peak particle flux is significantly shifted towards the HFS compared to the strike point position for the ISP.

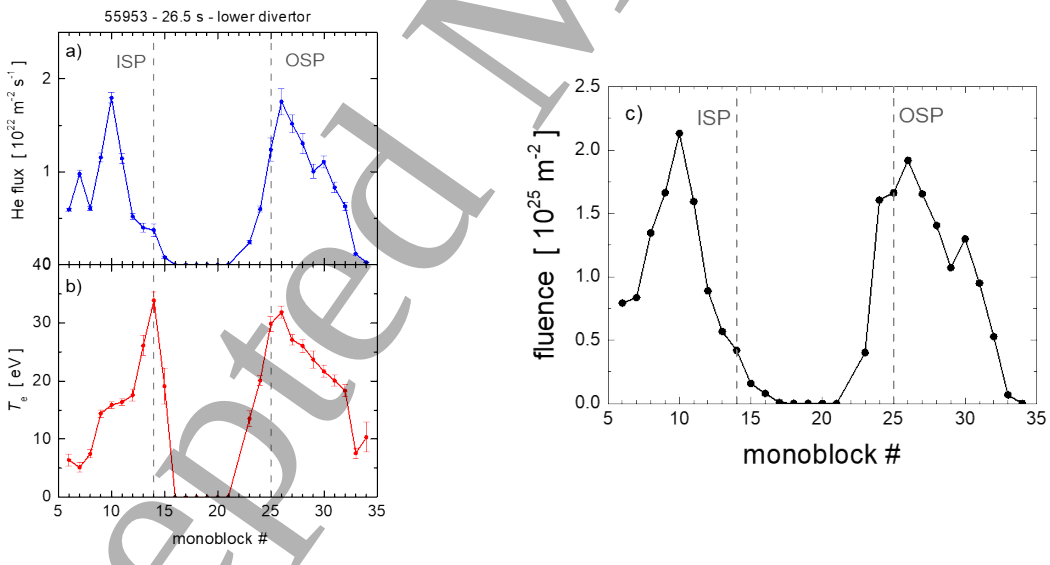


*Figure 3 : divertor plasma parameters as measured by Langmuir probes for a typical shot of the He campaign (#55953) with a) radial profile of the He incident particle flux and b) radial profile of the electron temperature. The He fluence cumulated over the He campaign (integrated between shots #55813 to #55987) is shown in c). Radial profiles are shown as a function of equivalent ITER like PFU monoblock (MB) number, with MB1 corresponding to the HFS and MB35 corresponding to the LFS, as illustrated in Figure 1. There are 12.5 mm between each probe. The position of the outer and inner strike points as inferred from magnetic reconstruction is also shown as dashed lines.*

Finally, these shots were also used to expose monocrystalline W samples to He plasmas, using a reciprocating collector probe. Around ~70 plunges of the collector probe were performed, cumulating He fluence in the range $10^{22}$-$10^{23}$ He/m$^2$. Results are not discussed in this paper but are reported in [17].

## 4. DISCUSSION ON TUNSGTEN FUZZ FORMATION IN WEST CONDITIONS

The key parameters playing a role in W fuzz formation, namely the incident He energy, the W surface temperature and the He fluence, are discussed below.

### 4.1. He incident energy

The He incident energy $E_{inc}$ can be derived from the Langmuir probe measurements, with $E_{inc} = 2\ T_i + 3\ Z\ T_e$ , where $T_i$ is the ion temperature, $T_e$ the electron temperature and Z the charge state of the ion (assuming a maxwellian distribution for the ions and a classical sheath acceleration).
Depending on the assumptions on $T_i$ and Z for He impinging on the surface, this yields an incident energy in the range 150-300 eV at the OSP based on the measured $T_e$ = 30 eV (corresponding to $T_i$=$T_e$ and Z=1 for the lowest range and $T_i$=2$T_e$ and Z=2 for the highest range).
According to [3], this should be high enough for W fuzz formation, and still below the energy at which W erosion becomes dominant over W fuzz formation. However, the higher limit in terms of energy (350 eV) given in [3] does not presumably take into account the impurity mix present in WEST plasmas, which are known to play a key role in W erosion for L mode plasmas [7][18][19].

### 4.2. He fluence

The He fluence can be estimated from integrating the He particle flux measured by the Langmuir probes over the whole campaign. The result is shown in Figure 3 c), with a fluence around 1.9 $10^{25}$ He/m$^2$ at the OSP, significantly above the seed fluence for W fuzz formation given in [3] ($10^{24}$ He/m$^2$).
It should be noted that assuming 100% of $He^{++}$ in the incident flux (as deduced from a calculation of the ion charge distribution as a function of electron temperature) corresponds to a lower limit for the calculation of the He flux and fluence, while it corresponds to a higher limit for the calculation of the He incident energy. Considering only singly charged $He^+$, as done for instance in [20], would multiply the He flux considered by a factor 2.
This calculation was performed assuming pure He plasmas impacting the divertor, but should not be strongly impacted by the trace D still present in the plasma, given the ratio He/($D_2$+He) > 90% measured in the exhaust gas. The impact of other intrinsic impurities present in WEST plasmas (such as a few % of carbon, oxygen or boron, see [18][19]) should be further refined, but should still result in a He fluence higher than the seed fluence for W fuzz formation. Indeed, taking into account the impact of 10% of D and 2-3% of an impurity with a charge state Z=6 would decrease the estimated He fluence by ~15%, to 1.7 $10^{25}$ He/m$^2$.
The important parameter to estimate however is which fraction of the total He fluence impacted the PFU at a surface temperature above the threshold for W fuzz formation (typically 700 °C or 973 K assumed here). This is discussed in the next paragraph.

### 4.3. PFU surface temperature

The evolution of the inertial PFU temperature as a function of space and time during the discharge can be estimated from IR measurements. This is illustrated in Figure 4, showing a top view of inertial divertor sectors as monitored by the IR system of WEST, with the area of maximum load indicated (labelled as max OSP).
Translating the black body temperature given by the IR system (corresponding to an emissivity $\varepsilon = 1$) to the real temperature of the divertor components requires assessing the local W emissivity. The emissivity for the W coated PFU has been measured before exposure in WEST and is ~0.15 for the temperature/wavelength range considered here [21]. However, the W emissivity has been evidenced to evolve strongly as a function of the surface state [21] and/or during plasma exposure [22]. A specific procedure has been applied in WEST to assess the divertor W emissivity evolution during experimental campaigns and is described in [22]. It was found that the emissivity in the OSP area does not vary strongly during the campaign, in contrast with emissivity in areas prone to deposition, and is ~0.12 at 200°C. In what follows, a variation of ± 20% of the W emissivity is taken around the value of pristine W coated PFU (corresponding to $\varepsilon = 0.15 \pm 0.03$ at 700°C), to account for possible changes during the campaign.

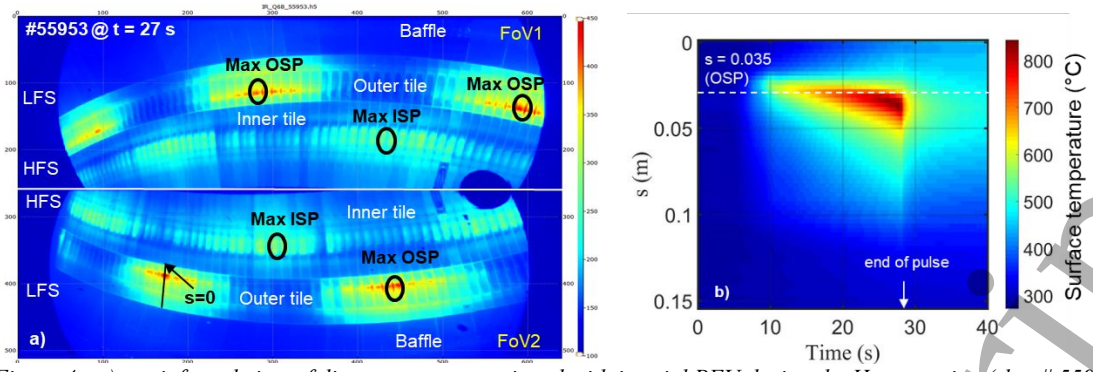


*Figure 4 : a) top infrared view of divertor sectors equipped with inertial PFU during the He campaign (shot # 55953 at t = 27s). The 2 field of view (FoV1 and FoV2) of the endoscope are shown on the top and the bottom of the picture (baffle and inertial PFU outer tile/inner tile indicated, see Figure 1). The pattern due to the ripple effect is seen, with the alternating maximum around the OSP / ISP indicated (black circle). The black line used to compute the temperature evolution presented on the right panel is also shown. It corresponds to the PFU located in the most loaded area in the ripple pattern. The temperature indicated on the left panel corresponds to black body (ε = 1). b) real surface temperature as a function of time and poloidal coordinate along the black line shown on the left figure (with s=0 corresponding to the HFS edge of the outer PFU in the PFR and s=0.035 m corresponding to the OSP position). The emissivity taken into account on the right panel is assessed as described in [22]*

The time evolution of the surface temperature at the max OSP derived from IR measurements is plotted in Figure 5 for ε = 0.15 ± 0.03. It is seen that a pulse length > 20 s is required to reach a PFU surface temperature above 700°C, where W fuzz formation can be expected. The plot on the right of Figure 5 illustrates the duration during which the W surface temperature was above 700°C in the OSP area throughout the He campaign, depending on the assumption on the W emissivity. It is seen that the region around the OSP (located at s=0.035m or MB25) was above the 700°C limit for ~100s during the He campaign for the reference W emissivity (most realistic case ε = 0.15, based on W emissivity measured in situ during the campaign and considering the emissivity increase with the temperature).

The time necessary to reach the seed He fluence of $10^{24}$ He/m$^2$ based on the Langmuir probe measurements is also shown as a horizontal dashed line (~140, 80 and 55 s for MB24, MB25 and MB26 respectively). For the most realistic case (W emissivity ε = 0.15), the threshold for W fuzz formation in terms of He fluence is reached in an area of ~1 cm width around the OSP. This would correspond to a He fluence of ~1.2 $10^{24}$ He/m$^2$ cumulated around the OSP above 700°C. It can be seen that the fraction of He fluence impacting the max OSP area at temperature above 700°C is only marginally above the seed He fluence, so that the tungsten fuzz thickness to be expected should be limited [3][23].

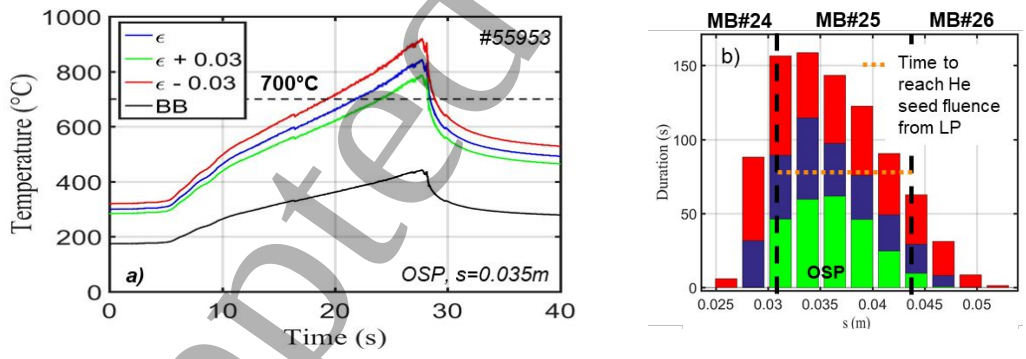


*Figure 5 : a) time evolution of the surface temperature of the inertial PFU at max OSP (at s=0.035 m along a PFU located in the most loaded area in the ripple pattern) as derived from IR measurements for shot # 55953. In black : black body temperature (ε =1), in blue real temperature for the reference emissivity of a pristine W coated PFU at 700°C (ε = 0.15) and in green and red for an emissivity range of ± 20% around the reference emissivity (ε=0.18 and 0.12 respectively). The dashed line indicates the 700°C limit above which W fuzz formation can be expected. b) cumulated duration above 700°C during the He campaign as a function of the poloidal coordinate along an inertial PFU located in the most loaded area in the ripple pattern. The equivalent monoblock number on an ITER like PFU is also given for reference. The duration is estimated for the 3 W emissivities considered in the left figure with the same color coding (ε = 0.18 in green, ε = 0.15 in blue, ε = 0.12 in red). The duration estimated to reach the seed He fluence for W fuzz formation ($10^{24}$ He/m$^2$) based on Langmuir probe measurement is also indicated as a horizontal dashed line for MB25.*

In the following section, first observations on the inertial PFU after the He exposure, concentrated in the max OSP area as described above, are reported.

## 5. FIRST OBSERVATIONS ON WEST PFU AFTER THE HE CAMPAIGN

### 5.1. In situ observations

In-vessel inspections using the Articulated Inspection Arm (AIA) of WEST, which allows internal components monitoring during campaigns without breaking the vacuum [24], were performed before and after the He campaign. The first inspection was carried out after the first day dedicated to the changeover from D to He and scenario optimization (12/11/2019) and the second one after the completion of the He campaign (18/11/2019). As shown in Figure 6, they did not reveal any macroscopic signs of W surface modification in the OSP area of inertial PFU, such as blackening of the surface reported when thick W fuzz is formed (see for instance [20]).

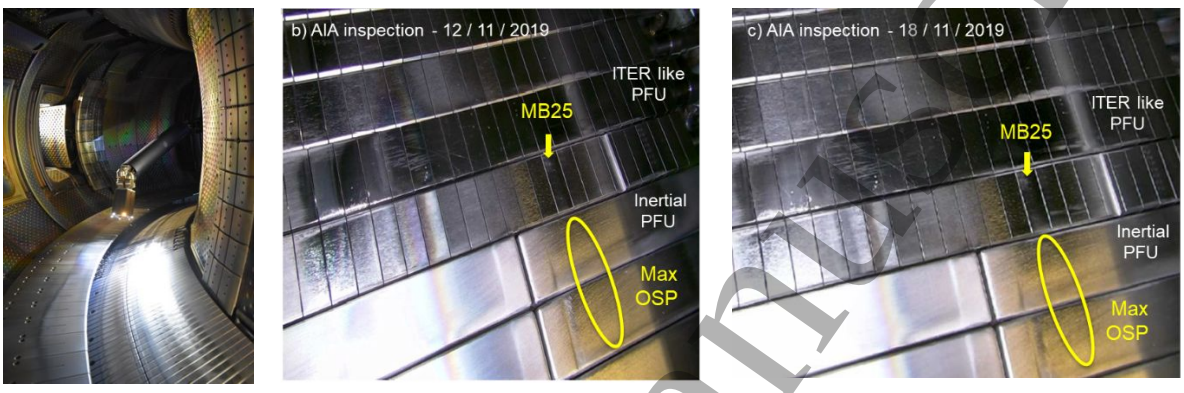


*Figure 6 : a) illustration of in vessel inspection using the Articulated Inspection Arm of WEST b) picture of the test divertor sector taken by the AIA before the He campaign, showing ITER like and inertial PFU. The area corresponding to the max OSP region on the inertial PFU is circled in yellow c) same picture taken by the AIA after the He campaign, showing no macroscopic signs of surface morphology changes in the area where W fuzz can be expected. ( ©V.Bruno/CEA )*

### 5.2. First insights from post mortem analysis

Post mortem analysis has started on erosion marker tiles exposed in the C3 and C4 campaigns. Full tiles have been analyzed using scanning electron microscopy (SEM) and focused ion beam (FIB) cross-sectioning in the large SEM AURIGA facility [8]. In complement, Rutherford Backscattering Spectrometry (RBS) was performed to assess the W erosion/deposition pattern through changes in the thickness of the different marker coatings.
By comparing reference areas on the erosion marker tiles (in position located in remote areas where no strong interactions with plasma is expected) with the max OSP area of the erosion marker tiles retrieved after the C3 and the C4 campaign respectively, no indications of W fuzz formation following the He campaign were found from SEM imaging / FIB cutting at this stage. From RBS and SEM data, the OSP area is found to be a net erosion zone after the C3 campaign, with an enlarged erosion zone identified after the C4 campaign.
More detailed investigations using a variety of post mortem analysis techniques are ongoing at the moment and should yield further insights on the plasma wall interactions processes at stake during the He campaign. In particular, the presence of He nanobubbles in the near surface will be investigated [25].
Based on the preliminary observations stated above, it can be speculated that in the conditions of the WEST He campaign, erosion was the dominating process over W fuzz formation in the max OSP area, in contrast with what could be expected from the criteria found in literature [3]. This shows the complementarity between experiments run in well controlled conditions in linear devices and experiments performed in the complex environment of fusion devices, where a number of competing processes need to be taken into account. In particular, the balance between W fuzz formation and other phenomena (such as W erosion/redeposition or W fuzz annealing under transients) is highly dependent on detailed tokamak conditions, such as the impurity mix present in the plasma, as they are known to dominate W erosion processes in L mode, the magnitude of local prompt W redeposition (at high magnetic field, eg 3.7 T in WEST) or the long range W redeposition coming from main chamber erosion.
Another point of interest when comparing results from linear devices and tokamaks is the time sequence of the He exposure, which was pulsed in the WEST conditions, with an evolving PFC surface temperature and He outgassing between plasma discharges, while linear devices work in most cases with steady state conditions, performing continuous He exposure at constant surface temperature. It should be noted however that [20] reported

consistent observations between W fuzz formed in a number of consecutive short pulses in Alcator C-Mod and linear devices run in a similar pulsed way.
Finally, recent modelling work [26] suggests that an incubation time, equivalent to the concept of a He incubation fluence, could play a role in the onset of W fuzz formation. This incubation time depends of the He exposure conditions (such as He incident flux, surface temperature …), and the associated characteristics of He implantation in W (such as He saturation level, He bubble size …). This model was validated against experiments performed under moderate He flux (~$10^{20}$ He/m$^2$/s) and long time exposure (up to 6 hours), and also compared to experiments in PISCES-E at higher He incident flux (~$10^{21}$ He/m$^2$/s). It would be interesting to check whether, according to this model, the time spent above the PFC surface temperature threshold for each discharge (up to ~10s) is expected to be a limiting factor for W fuzz formation in WEST conditions (He incident flux ~$10^{22}$ He/m$^2$/s ). It should be reminded however that under high He incident flux conditions (>$10^{24}$ He/m$^2$/s), a short exposure time above the surface temperature threshold (~1s for each of the consecutive 14 discharges) did not prevent W fuzz formation in the Alcator C-Mod experiment reported in [20].

## 6. SUMMARY AND PROSPECTS

A dedicated He-W PWI experiment was performed in WEST, with 2000s of repetitive pulses and a fluence up to 3.5 $10^{25}$ He/m$^2$ on the lower divertor. Conditions for W fuzz formation as derived from linear devices experiments ($E_{inc}$ > 20 eV, fluence > $10^{24}$ He/m$^2$, $T_{surf}$ > 700°C) were met in the outer strike point area of the inertial W coated PFU. However, based on combined IR and Langmuir probe measurements, the fraction of the He fluence impacting the PFU at a surface temperature above 700°C was only marginally above the seed He fluence required for W fuzz formation. Preliminary inspection of the components after the campaign did not show visible signs of surface modification. An extensive post mortem analysis is now ongoing to confirm these first indications.
These results underline that in tokamak conditions, the complex balance between W erosion (in particular from impurities) /redeposition (from W eroded from the main chamber or from prompt redeposition) and W fuzz formation needs to be taken into account, as was shown in other tokamak experiments [27] [28][29]. The data obtained will be used to consolidate the experimental database supporting the modelling effort for predicting W fuzz formation and growth in ITER, such as in [30].
WEST is now entering its second phase of operation, with a full actively cooled ITER like divertor. This will enable the full long pulse capability of WEST, and allow further dedicated campaigns to be run at significantly higher fluence in both deuterium and helium plasmas.

## ACKNOWLEDGEMENTS

This work has been carried out within the framework of the EUROfusion Consortium and has received funding from the Euratom research and training programme 2014-2018 and 2019-2020 under grant agreement No 633053. The views and opinions expressed herein do not necessarily reflect those of the European Commission. Part of this work was performed under EUROfusion WP PFC.

## REFERENCES

[1] PITTS R. et al., Physics basis for the first ITER tungsten divertor, Nucl. Mater. Energy **20** (2019) 100696.
[2] ITER Research Plan within the Staged Approach, ITR-18-003, 2018
[3] DE TEMMERMAN G. et al., The influence of plasma-surface interaction on the performance of tungsten at the ITER divertor vertical targets, Plasma Phys. Control. Fusion 60 (2018) 044018
[4] BUCALOSSI J. et al., The WEST project: Testing ITER divertor high heat flux component technology in a steady state tokamak, Fusion Eng. Des. 89 907 (2014)
[5] MISSIRLIAN M. et al., The WEST project: Current status of the ITER-like tungsten divertor, Fusion Eng. Des. 89 1048 (2014)
[6] FIRDAOUSS M. et al., Operational limits on WEST inertial divertor sector during the early phase experiment, Phys. Scr., 2016 (2016), Article 014012
[7] HAKOLA A. et al., Gross and net erosion balance of plasma-facing components in full-W tokamaks, 28th IAEA Fusion Energy Conference (Proc. Int. Conf., Nice, France, 2021), accepted for publication in Nuclear Fusion Journal
[8] BALDEN, M., et al., Erosion and redeposition patterns on entire erosion marker tiles after exposure in the first operation phase of WEST, PFMC 2021, accepted for publication in Phys. Scripta
[9] COURTOIS X. et al., Design and status of the new WEST IR thermography system, Fusion Engineering and Design Volume 136, Part B, November 2018, Pages 1499-1504

[10] HOURY M. et al., The very high spatial resolution infrared thermography on ITER-like tungsten monoblocks in WEST Tokamak, Fusion Engineering and Design, Volume 146, Part A, September 2019, Pages 1104-1107
[11] CORRE Y. et al., Integration of fiber Bragg grating temperature sensors in plasma facing components of the WEST tokamak, Rev. Sci. Instrum., 89 (2018), Article 063508
[12] GASPAR J. , et al. First heat flux estimation in the lower divertor of WEST with embedded thermal measurements, Fus. Eng. Des., 146 (2019), pp. 757-760
[13] DEJARNAC R. et al., Flush-mounted Langmuir probes in the WEST tokamak divertor, Fusion Engineering and Design Volume 163, February 2021, 112120
[14] GASPAR J. et al., Divertor power loads and scrape off layer width in the large aspect ratio full tungsten tokamak WEST, 28th IAEA Fusion Energy Conference (Proc. Int. Conf., Nice, France, 2021), 2021 Nucl. Fusion 61 096027
[15] BISSON, R. et al., Deuterium and helium outgassing following plasma discharges in WEST: Delayed D outgassing during D-to-He changeover experiments studied with threshold ionization mass spectrometry, Nuclear Materials and Energy, Volume 26, March 2021, 100885
[16] MAGET P. et al., How Nitrogen seeding securizes plasma ramp-up in the metallic environment of WEST, EPS2020-2021
[17] WIRTH B. et al., Measuring and modeling helium accumulation in single crystal tungsten specimens exposed to He plasma discharges in the WEST reciprocating collector probe, 28th IAEA Fusion Energy Conference (Proc. Int. Conf., Nice, France, 2021), Preprint: 2020 IAEA Fusion Energy Conference, Nice (2021), EX/P5-3
[18] VAN ROOIJ, G., et al., Tungsten divertor sources in WEST related to impurity inventory and local plasma conditions, Phys. Scr. **T171** (2020), 014060.
[19] GALLO, A. et al., Interpretative transport modeling of the WEST boundary plasma: main plasma and light impurities, Nucl. Fusion **60** (2020), 126048
[20] G.M. Wright at al., Comparison of tungsten nano-tendrils grown in Alcator C-Mod and linear plasma devices, Journal of Nuclear Materials, Volume 438, Supplement, July 2013, Pages S84-S89
[21] GASPAR J. et al., Emissivity measurement of tungsten plasma facing components of the WEST Tokamak, Fusion Eng. Des., 149 (2019), Article 111328
[22] GASPAR J. et al., In-situ assessment of the emissivity of tungsten plasma facing components of the WEST tokamak, Nuclear Materials and Energy, Volume 25, December 2020, 100851
[23] PETTY T. et al., Tungsten 'fuzz' growth re-examined: the dependence on ion fluence in non-erosive and erosive helium plasma, l 2015 Nucl. Fusion 55 093033
[24] BRUNO V. et al., WEST regular in-vessel Inspections with the Articulated Inspection Arm robot, Fusion Engineering and Design 2019, Volume 146, Part A, September 2019, Pages 115-119
[25] MARTIN C. et al., First post-mortem analysis of deposits collected on ITER-like components in WEST after the C3 and C4 campaigns, PFMC 2021, accepted for publication in Phys. Scripta
[26] Chao-Shou Chen et al, Effects of elastic softening and helium accumulation kinetics on surface morphological evolution of plasma-facing tungsten, 2021 Nucl. Fusion 61 016016
[27] BREZINSEK, S., et al., Surface modification of He pre-exposed tungsten samples by He plasma impact in the divertor manipulator of ASDEX Upgrade, Nucl. Mater. Energy **12** (2017), 575-581.
[28] HAKOLA, A., et al., Plasma-wall interaction studies in the full-W ASDEX upgrade during helium plasma discharges, Nucl. Fusion **57** (2017), 086019.
[29] BREZINSEK, S., et al., "The competition between metallic nanostructures formation, erosion and co-deposition in He plasmas of the tokamaks EAST, WEST, and ASDEX Upgrade", 24th International Conference on Plasma Surface Interactions in Controlled Fusion Devices (PSI 2020) (Proc. Int. Conf., Jeju, Korea, 2021).
[30] DE TEMMERMAN G. et al., A growth/annealing equilibrium model for helium-induced nanostructure with application to ITER, Nuclear Materials and Energy 19 (2019) 255–261256